

A toy model provably featuring an arrow of time without past hypothesis

Pablo Arrighi 

Université Paris-Saclay, Inria, CNRS, LMF, 91190 Gif-sur-Yvette, France
IXXI, Lyon, France

Gilles Dowek 

Université Paris-Saclay, Inria, CNRS, LMF, 91190 Gif-sur-Yvette, France

Amélia Durbec 

Université Paris-Saclay, CNRS, LISN, 91190 Gif-sur-Yvette, France

Abstract

The laws of Physics are time-reversible, making no qualitative distinction between the past and the future—yet we can only go towards the future. This apparent contradiction is known as the ‘arrow of time problem’. Its resolution states that the future is the direction of increasing entropy. But entropy can only increase towards the future if it was low in the past, and past low entropy is a very strong assumption to make, because low entropy states are rather improbable, non-generic. Recent works, however, suggest we can do away with this so-called ‘past hypothesis’, in the presence of reversible dynamical laws featuring expansion. We prove that this is the case for a toy model, set in a $1+1$ discrete spacetime. It consists in graphs upon which particles circulate and interact according to local reversible rules. Some rules locally shrink or expand the graph. Generic states always expand; entropy always increases—thereby providing a local explanation for the arrow of time.

2012 ACM Subject Classification Theory of computation → Quantum information theory

Keywords and phrases Causal graph dynamics, Janus point, Big bounce crunch and bang, Typicality

Funding This project/publication was made possible through the support of the ID# 62312 grant from the John Templeton Foundation, as part of the ‘The Quantum Information Structure of Spacetime’ Project (QISS). The opinions expressed in this project/publication are those of the author(s) and do not necessarily reflect the views of the John Templeton Foundation.

Acknowledgements We wish to thank Marios Christodoulou, Pierre Guillon, Benjamin Hellouin, Carlo Rovelli and Francesca Vidotto for many discussions and insights.

1 Introduction

The main contribution of this paper is the first rigorous proof that an arrow of time typically emerges in some reversible dynamics, without the need for a past hypothesis. Whilst the motivations of the question asked lie in fundamental Physics, the methods of the answer given lie theoretical Computer Science (models of computation, invariants, termination proof, some information theory). The toy model is also explored numerically, as well as natural variants.

Physics laws are time-reversible, i.e. time evolution can be inverted, making no qualitative distinction between the past and the future. Yet, we clearly experience the fact that we cannot go back to the past, this is referred to as the ‘arrow of time problem’. The paradox is resolved by considering different quantities as ‘clocks’, and then identifying the future direction to be direction of increase of a certain, physically-defined clock, thereby providing a time arrow. Usually, this quantity is an entropy, and one shows that starting from a low entropy initial state, it typically increases even under a reversible law. Thus, in the conventional argument due to Boltzmann [12], “reversible dynamical law + past low entropy

⇒ arrow of time”. This argument works even for systems of bounded size (e.g. a few of particles in a box). But it suffers three important criticisms: (i) By the Poincaré recurrence theorem, as we iterate the dynamics forward, the entropy typically increases... but then drops back, and increases, etc., as the dynamical system is necessarily periodic. The criticism is usually dismissed on the base that the recurrence period is beyond cosmological times. (ii) Starting from an initial low entropy state and iterating the dynamics forward, entropy typically increases (“entropic clock’s arrow” matches that of the external time-coordinate aka “dynamical clock”). However, had we applied the reversed dynamics instead, iterating the dynamics backward, entropy typically would have increased, too (the entropic clock’s arrow does not match the dynamical clock’s arrow) [18], as is quite often overlooked. (iii) The assumption that the initial state be of low entropy, also referred to as ‘the past hypothesis’ [1] is a very strong one. This is because generic state have maximal entropy. Hence, the presence of such an improbable state at dynamical clock time 0, remains a mystery. We will review these points in Sec. 2.

In [14, 15], Carroll and Chen try to fix the third criticism and provide the first plausible explanation whereby “reversible dynamical law ⇒ arrow of time”. Their key new ingredient is big bounce (big crunch then bang) then eternal expansion (as featured also in several early attempts to restore a particle physics symmetry called CPT at the scale of the universe [25, 13]). Their model is left informal however, leaving plenty of room to discuss whether it really manages to do away with the past hypothesis [28, 27, 29]. In particular, they themselves raise the issue whether expansion is actually compatible with reversibility.

Informally, in a big bouncing universe, matter gets compressed by the big crunch, and released by the big bang. Expansion happens so fast that matter then finds itself out of equilibrium, in a low entropy state. Matter then diffuses and entropy increases without ever reaching a maximum, as expansion is eternal. The entropic clock’s arrow thus matches that of the “size-of-the-universe clock”, which in turn matches that of the dynamical clock after the big bounce. This explanation is compelling. Yet the following direct logical consequence is somewhat mind-bending: before the big bounce occur, the size-of-the-universe clock, and thus the entropic clock, have their arrow opposite to that of the dynamical clock. In dynamical clock time we may be seating here reading this paper ∼ 13.7 billion years after the big bounce, whilst others may be doing the same ∼ 27.4 billion years ago facing the opposite direction—these twin entropic times facing each other have in fact been popularized as ‘Janus time’ by Barbour [9]. Still, as counter-intuitive as it may be, this is already happening in the conventional argument by Boltzmann: as pointed out by Golstein et al. [18], this is just the mentioned criticism (ii). Moreover general relativity teaches us to be weary of the physical meaning we attach to coordinates: it may be that in dynamical clock time coordinates—for instance in the so-called no-boundary solutions, there is “no time” at the big bounce [20].

Barbour et al. [9, 10] use the n –body problem, with (non-local) Newtonian classical gravity turned on, as an enlightening analogy of big-bounce-then- eternal-expansion. The question whether this model really does away with the past hypothesis has been argued in [30]. Indeed as the considered bodies travel on a pre-existing infinite space, the analogy blurs out the requirement of finite but unbounded configurations, which is needed to make the argument rigorous. Moreover, the entropic clock (measure of increasing microscopic disorder) is replaced by a “shape complexity clock” (measure of increasing macroscopic clumping) in these works. This is non-standard and arguable on the basis that in many situations there is no need for gravitational clumping in order to observe an arrow of time, e.g. at cosmological scales or at microscopic scales. Matter clumping mainly helps delay thermal death, as we shall see. The question whether expansion can be implemented as a local reversible physical

laws also remains open in this strand of works [22].

The aim of this paper is to exhibit rigorously-defined local reversible dynamical laws (alike a lattice gas automaton) for which we can prove that, for a rigorously-defined notion of entropy (alike that of perfect gas):

- Generic states always end up growing in size as we iterate the dynamics.
- Entropy always increases as size grows.

Thus we prove that an entropic clock direction emerges without the need to assume past low entropy. In other words the arrow of time is established from local reversible expansion mechanisms alone, doing away with the past hypothesis. Again, this works because size as a function of dynamical clock time is typically *U*-shaped. As generic states are somewhere on this *U*-curve, their size will end up growing, and their entropy will end up increasing. They will do so forever, as configurations are of finite but unbounded size. Of course generic states have, somewhere along the dynamical clock timeline, some states of smallest size and lowest entropy, which may be dubbed as “initial”. These particular states are non-generic, just like the minimum of any *U*-curve is non-generic. Because the *U*-curve is due to the dynamics alone, their existence is the result of dynamics alone.

Our toy model is set in 1+1 spacetime. It consists in circular graphs upon which particles move and interact when they are closeby. Moreover, local some patterns are interchanged, triggering shrinking or expansion of the circle. It is inspired by the Hasslacher-Meyer model, for which there is numerical evidence of a *U*-shaped size curve, but no proof—this seems inherently hard to prove in fact. There is no mention of the arrow of time nor entropy in their paper [21]; moreover the sense in which it is reversible and causal is left informal and seems incompatible with quantum mechanics [3]. Instead, our toy model enjoys rigorous proofs of *U*-shaped size and entropy curves, as well as rigorous notions of reversibility [5] and causality (i.e. making sure that information propagates at a bounded speed with respect to graph distance), readily allowing for a quantum extension [4]. These results are provided in Sec. 3.

Much Physics is not only time-reversible but also time-symmetric, i.e. invariant under the change of variable $t = -t'$, thereby making no distinction at all between the past and future time directions. We provide numerical evidence that there is a time-symmetrized extension of our model that has *U*-shaped size curve and entropy curves in Sec. 4.

The toy model features quadratic expansion, whereas the very early universe is believed to have experienced a short exponential expansion phase referred to as ‘inflation’. We provide numerical evidence that a slight variant of the toy model features an exponential *U*-shaped size curve in Sec. 5.

The toy model features quick ‘thermal death’. Once thermal death is reached, the arrow of time can no longer be witnessed locally. We provide numerical evidence that just by adding inelastic collisions of matter to the model (and triggering the emission of radiation into free space so as to keep things reversible) thermal death gets delayed, see Sec. 6.

Summary and perspectives are given in Sec. 7.

2 The conventional argument

Entropy. Entropy was defined by Boltzmann[11] in the 1870s:

► **Definition 1.** *The entropy S of a macroscopic state is defined by :*

$$S = k \cdot \ln \Omega$$

with k the Boltzmann constant and Ω is the number of microscopic configurations corresponding to the macroscopic state.

Intuitively, the ‘macroscopic state’ refers to a set of values for the macroscopic properties of the system, such as its temperature, pressure, volume or density.

Given a certain macroscopic state, a ‘statistical ensemble’ is a way to assign a probability distribution over the set of microscopic states that correspond to the macroscopic state. It is often reasonable to assume that the probability distribution be uniform (aka a ‘microcanonical ensemble’). The probability p_i of a microscopic state x_i is then $p_i = \frac{1}{\Omega}$. The connection between the Shannon entropy [26] of this probability distribution, and the Boltzmann entropy of the macrostate, is then obvious:

$$S = -k \sum_{i=0}^{\Omega-1} p_i \ln(p_i) = -k \sum_{i=0}^{\Omega-1} \frac{1}{\Omega} \ln\left(\frac{1}{\Omega}\right) = k \cdot \ln \Omega$$

For a dynamical system over the state space X , the microscopic states are simply the configurations $x_i \in X$ of the system. We formalize the macroscopic states as equivalence classes on X . The entropy function associates, to each microscopic state, the entropy of its macrostate.

► **Definition 2.** Consider X a set and \equiv an equivalence relation on X . We define the entropy function $S_\equiv : X \rightarrow \mathbb{R}$ associated with \equiv as:

$$S(x) = \ln(|[x]|)$$

with $[x]$ the \equiv -equivalence class of x and $|[x]|$ is its size.

The case of bounded size dynamical systems. The second principle of thermodynamics states that entropy increases in time. However, even for closed, bounded size dynamical systems, the situation is not so obvious:

► **Remark 2.1.** Let X be a finite state space and $f : X \rightarrow X$ a bijection. For any entropy function S , and for any configuration $x \in X$, the sequence $(S(f^n(x)))_{n \in \mathbb{N}}$ is periodic because the sequence $f^n(x)_{n \in \mathbb{N}}$ is periodic. This implies that the sequence of entropy variations $(S(f^{n+1}(x)) - S(f^n(x)))_{n \in \mathbb{N}}$ is itself periodic. If $(S(f^n(x)))_{n \in \mathbb{N}}$ is not constant, then these entropy variations can be negative.

How can we justify, then, that when we dilute a drop of dye in a sealed glass of water, entropy seems to just rise, unambiguously indicating an arrow of time? Actually several assumptions are implicit this emblematic experiment.

First, the duration of such an experiment likely to be far too short to observe periodicity. To give an order of magnitude, for a molar volume of $22.4L$ of perfect gas, the number of microstates Ω is $\sim 10^{5 \times 10^{24}}$. Intuitively, the period ought to be of that same order of magnitude, as expressed in units of Planck time (minimal observable time). However, it is estimated that only 10^{60} Planck times have elapsed since the Big Bang.

Second, the drop of dye would likely have diluted just as well if it had undergone the time-symmetrized versions of Physics laws instead. In other words, entropy typically does increase when we start from a low entropy initial configuration... but it does so in both directions of the dynamical clock [18].

Third, we must realise that the experiment starts off at a rather improbable time: the first 10^{60} ticks of dynamical clock time represent a negligible fraction of $\sim 10^{5 \times 10^{24}}$ entropy

period. Had current time been picked up at random within the period, there would be no reason to suppose to expect it to be a time of increase of entropy, rather than of decrease. Another way to say this is that the experiments starts off from an improbable configuration. Indeed in any generic configuration the dye is diluted already; entropy is almost maximal already; and the entropy variation is zero on average, independently of t the number of steps between the two observations:

$$\sum_{x \in \Sigma} (S(f^t(x)) - S(x)) = \sum_{x \in \Sigma} S(x) - \sum_{x \in \Sigma} S(x) = 0.$$

In order to witness an arrow of time, we must start from a low entropy configuration, but in practice the equivalence relation and therefore the entropy function are chosen so that low-entropy configurations are non-generic.

Past hypothesis. Still, to this day, phenomena such as the dilution of the drop of dye in a glass of water, and the increasing entropy therein, are paradigmatic of our resolution of the arrow of time problem. In a sense, this only displaces the problem. The question “Why do we observe an arrow of time” has become “Why was the Universe originally of low entropy?”. The conventional argument requires that the entropy at the Big Bang be so low enough that an arrow of time is still observable ~ 13.7 billion years later—making it a very strongly non-generic configuration. This strong assumption of a low entropy initial configuration is referred to as the ‘past hypothesis’ [1], and was criticised right from its birth, on account of this unlikelihood [12]. Luckily, more recent accounts of the arrow of time suggest we could do without it [14, 15, 9, 8]. The key ingredient is expansion.

3 Arrow of time without past hypothesis

In this section we prove via a toy model that an entropic arrow of time can originate from expansion, and that this expansion can be implemented locally and reversibly. In the model remark 2.1 does not apply because, although each configuration is finite, the state space itself is infinite, as configurations can grow. This is not surprising by itself: think of \mathbb{N} the set of integers for instance. Each number can be written with a finite number of digits, but the set itself is of course infinite, and it is easy to define a non-periodic bijection on the set:

$$f(n) = \begin{cases} 0 & \text{if } n = 1 \\ n + 2 & \text{if } n \text{ is even} \\ n - 2 & \text{else} \end{cases}$$

What is much less obvious is the existence of a reversible, causal, homogeneous, ultimately expanding dynamics on generic configurations.

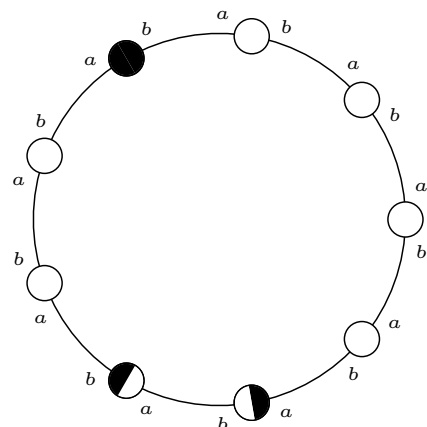
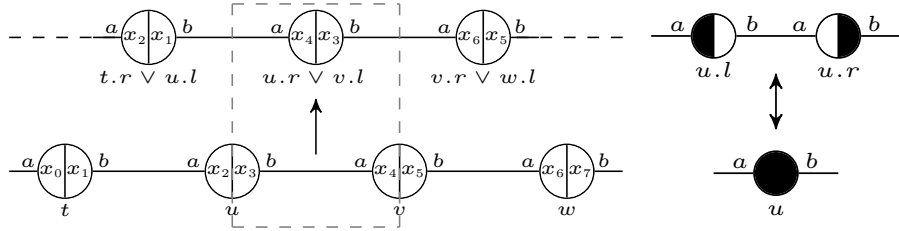


Figure 1 A configuration. Each full half-disks represents the presence of an (undistinguishable) particle that is about to hop along the corresponding port.



(a) *Step $\sqrt{\tau}$.* Each particle hops by half an edge. In other words, edges become vertices and vertices become edges. Particles keep their orientation.

(b) *Step I.* All occurrence of the two patterns are flipped for the other synchronously. This can be done without ambiguity, as the patterns do not overlap.

Figure 2 Rules of the toy model.

3.1 State space

The states of the model are circular graphs of 1 dimension. These circles are of unbounded but finite size, i.e. the line is not allowed. The vertices are equipped with ports a and b , and edges go from port to port, each being used exactly once, as in Fig. 1.

Each vertex carries an internal state, amongst four possible states: ‘containing no particle’, ‘containing a particle moving along port a ’, ‘containing a particle moving along port b ’, ‘containing two particles’. Notice that this set of internal states is the same as that used to model electrons in gas-on-grid methods [19], or in quantum walks to represent the spin of a fermionic particle such as the electron [2]. Later we will generalize this by associating, to each port of each node, not just one information bit, but two or three.

There is one subtlety: vertices are named, and these names form a little algebra. This is so that a vertex u may be able to split into $u.l$ and $u.r$, and later merge back into $u.l \vee u.r$, and that this be in fact the same as just u . There is no escaping this formalism in order to achieve both reversibility and local vertex creation/destruction [6], particularly if one wants to preserve causality in the quantum regime [3]. To maintain full rigour and remain self-contained, the full definition of these named graphs is provided in Appendix A.

We denote by \mathcal{C}_n the set of circular graphs with $2n$ information bits per vertex (n per port). For any vertex x , we denote by $p_i(x)$ the value of the i -th bit of the port p of vertex x .

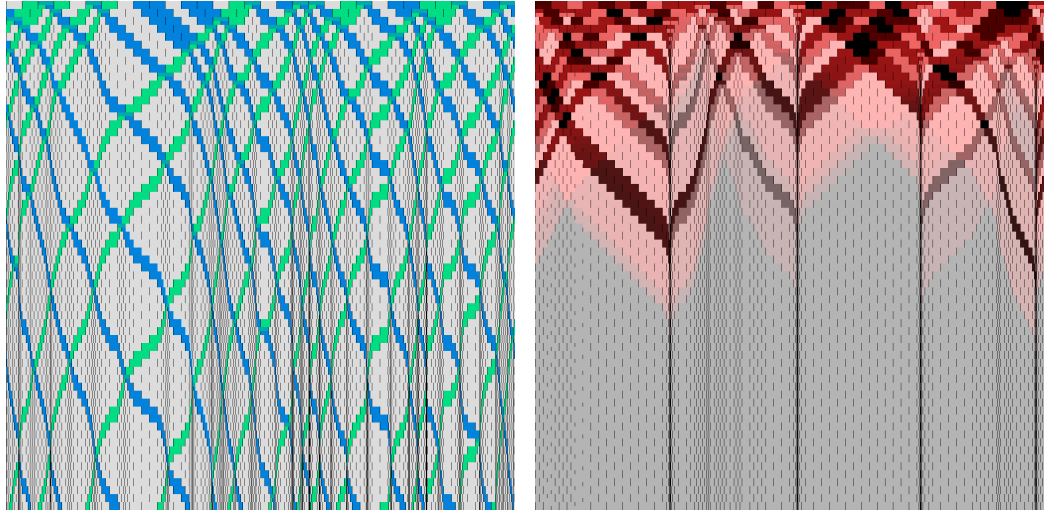
3.2 The toy model

Our main model ($\sqrt{\tau}I$) is inspired by the Hasslacher-Meyer dynamics [21]. It acts on the set \mathcal{C}_1 and consists in composing two steps: I , then $\sqrt{\tau}$. The whole dynamics is time-reversible. It consists in a composition of steps which, taken individually, are time-symmetric [17]:

► **Definition 3.** *A causal graph dynamics f , it is said to be time-symmetric if and only if there exists a causal graph dynamics T such that $T^2 = Id$ and $TfT = f^{-1}$.*

Step $\sqrt{\tau}$. Let τ be the operation that moves all particles along their corresponding port. The operation $\sqrt{\tau}$ is such $\sqrt{\tau} \circ \sqrt{\tau} = \tau$: it moves particles by half an edge instead, see Fig. 2a. One way of thinking about this operation is as inverting the roles of edges and nodes in the sense of taking the dual graph. Notice that alternatively, we could have used a (renaming-equivalent but less symmetrical) operation that moves only those particles associated to port b , but by a whole edge.

► **Definition 4 ($\sqrt{\tau}$).** *Step $\sqrt{\tau}$ is defined for any graph $X \in \mathcal{C}_n$ as follows:*



(a) Spacetime diagram of dynamics $\sqrt{\tau}I$. Dynamical clock time flows towards the bottom. Particles corresponding to port a (resp. b) are represented green (resp. blue). Intermediate steps I are also shown.

(b) Spacetime diagram and local entropy of dynamics $\sqrt{\tau}I_2$. Particles are shown in levels of grey, local entropy is shown in levels of red.

- $V(\sqrt{\tau}(X)) = \{u.r \vee v.l \mid \{u : b, v : a\} \in E(X)\}$
- $E(\sqrt{\tau}(X)) = \{\{x' : b, y' : a\} \mid u, x, y \in V(X) \text{ et } x' = u.r \vee x.l \text{ et } y' = y.r \vee y.l\}$
- $\forall x' \in V(\sqrt{\tau}(X)), \text{ and for all } i \in [1, n], a_i(x) = a_i(u) \text{ and } b_i(x) = b_i(v), \text{ where } u \text{ and } v \text{ are the vertices of } X \text{ such that } x'.l = u.r \text{ and } x'.r = v.l \text{ respectively.}$

This step is both reversible and time-symmetrical, since

$$\sqrt{\tau}^{-1} = T\sqrt{\tau}T$$

with T the function exchanging the left and right information bits of each vertex.

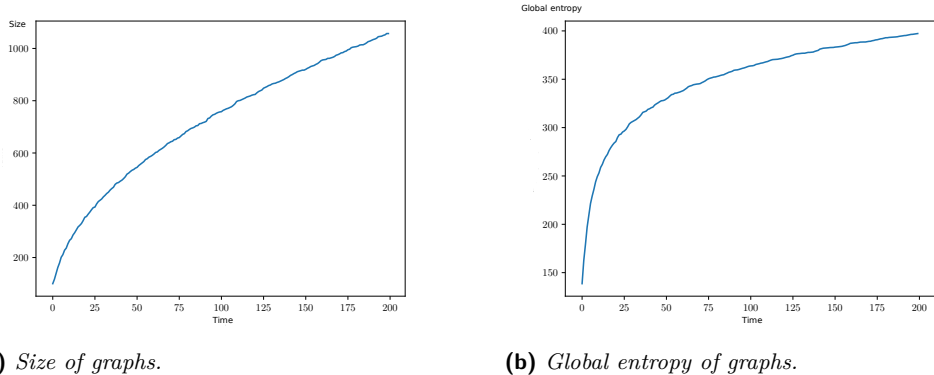
Step I. Step I consists in splitting a vertex into two when it holds two particles, or conversely merging two vertices holding a pair of back-to-back particles, as in Fig. 2b. Thus, a vertex u such as $a_1(u) = b_1(u) = 1$ will produce two vertices $u.l$ and $u.r$ with $a_1(u.l) = b_1(u.r) = 1$ and $b_1(u.l) = a_1(u.r) = 0$. Conversely, two vertices u and v , with $a_1(u) = b_1(v) = 1$ and $b_1(u) = a_1(v) = 0$ will merge into a vertex $u \vee v$ such as $a_1(u \vee v) = b_1(u \vee v) = 1$.

This step is obviously reversible and time-symmetric, since it is involutive: $I^2 = Id$.

Spacetime diagram. The evolution of a configuration under toy model $\sqrt{\tau}I$ can be represented in the form of a spacetime diagrams, e.g. Fig. 3a represents $\sqrt{\tau}I$. In these diagrams, the spatial dimension is represented horizontally, and dynamical clock time is represented vertically downwards. Each vertex is represented by a cell, separated from its neighbours with a vertical black line. Its internal state of a cell is captured by its colour. The cells are depicted in variable-sizes, allowing each split/merge to be done “on the spot”.

3.3 Size increases

The first observation that can be made from Fig. 3a is that the dynamics $\sqrt{\tau}I$, although reversible, grows the size of the graph. It does not grow from the borders, there are no



■ **Figure 4** Typical size and entropy curves for dynamics $\sqrt{\tau}I$. The horizontal axis represents the number of steps of the dynamics, aka dynamical clock time. The initial configuration is drawn uniformly at random amongst all graphs of size 100.

borders, it just expands locally. The numerics in Fig. 4a suggest this is typical. We will now prove that this happens for generic initial states. In fact, we will prove the stronger result that graphs always end up growing, and that the growth is strict as soon as they contain at least one particle of each type.

Intuitively this is due to the fact that vertex merger only occurs in the presence of a pattern which is unstable:

► **Lemma 5** (Merger Instability). . Let be a circular graph $X \in \mathcal{C}_1$. Given a pair u and v of adjacent vertices of X , these are said to belong to a merger pattern if and only if $a_1(u) = b_1(v) = 1$ and $b_1(u) = a_1(v) = 0$. For any $u v$ forming a merger pattern in X , there are two vertices $u.r, v.l \in V((\sqrt{\tau}I)^{-1}(X))$ such that $u.r$ and $v.l$ form a merger pattern.

Proof. By inspection of Fig. 5, which represents the pre-image of a merger pattern. ◀

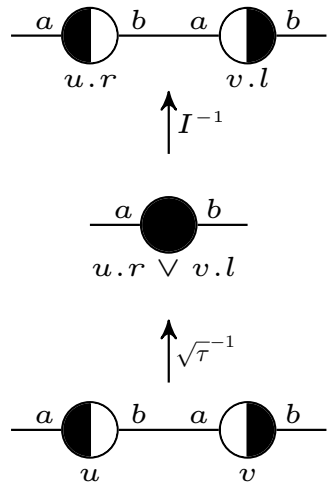
Let us fix notations before we state the expansion theorem. first; in what follows we will write (u_n) to designate the sequence $(u_n)_{n \in \mathbb{N}}$ in the absence of ambiguity and use:

► **Definition 6.** Let there be two sequences (u_n) and (v_n) . We say that (u_n) is of the order of (v_n) , and write $(u_n) = \Theta((v_n))$ if there exist $a, b \in \mathbb{R}$ and $n_0 \in \mathbb{N}$ such that for all $n \geq n_0$, $a.v_n \leq u_n \leq b.v_n$.

We have:

► **Theorem 7** (Expansion). For any $X \in \mathcal{C}_1$ containing at least one particle of each type, $(|V((\sqrt{\tau}I)^n(X))|) = \Theta((\sqrt{n}))$.

Proof. (Outline). By Lem. 5 dynamics $\sqrt{\tau}I$ cannot create a merger pattern and these are destroyed on the slightest collision. Essentially, there remains to prove that such collisions will occur and destroy all merger patterns. The proof technique is thus akin to a program termination proof. It is technical, we shift it to Appendix B for readability. ◀



■ **Figure 5** Instability of merger patterns under $\sqrt{\tau}I$.

As can be seen in Fig. 4a, for a randomly chosen configuration, the asymptotic regime is reached quickly and is quite stable.

3.4 Entropy increases with size

It turns out that growth in the size of the graph implies growth of entropy, for a natural notion of entropy.

Indeed from this point on, we will focus on the entropy function associated with the following equivalence class: two configurations are considered equivalent if and only if they have the same size and the same number of particles. This entropy function can be seen as analogous to the one used in the study of perfect gases.

This is because the entropy of a perfect gas configuration is generally associated with the macroscopic properties of pressure, volume, temperature and number of particles. As these four variables are related by the perfect gas law, three are independent. Moreover, in our toy model the speed of the particles is constant, which makes it unnecessary to consider the temperature. We therefore have to consider just two variables amongst: the number of particles; the size of the graph (analogous to the volume); and the density of particles (analogous to the pressure).

We ignore the names of the vertices when counting the microstates corresponding to the macrostates, i.e. when counting the number of graphs of a given size and having a given number of particles. We denote $\binom{n}{p}$ the binomial coefficient p among n , i.e. $\binom{n}{p} = \frac{n!}{p!(n-p)!}$.

► **Definition 8.** *The entropy function S' is defined by $S'(X) = \log(\binom{|V(X)|}{p})$ where p is the number of particles in X .*

In the case of $\sqrt{\tau}I$ we have proven in Th. 7 that $V(X)$ grows as a square root. Because this rule preserves the number of particles we automatically obtains the growth of entropy. But we can be more precise:

► **Corollary 3.1.** For any $X \in \mathcal{C}_1$ containing at least one particle of each type, $(S'(\sqrt{\tau}I)^n(X))_{n \in \mathbb{N}} = \Theta((\log(n)))$.

Proof. Thanks to Th. 7, we have that $(S'(\sqrt{\tau}I)^n(X))_{n \in \mathbb{N}} = \Theta(\log(\binom{\Theta(\sqrt{n})}{p}))$ Using the bounds $(\frac{a}{b})^b \leq \binom{a}{b} \leq e^b(\frac{a}{b})^b$ [16], and noting that p is constant, we obtain :

$$(S'(\sqrt{\tau}I)^n(X))_{n \in \mathbb{N}} = \Theta(p \log(\frac{\Theta(\sqrt{n})}{p})) = \Theta(\log(n^{1/2})) = \Theta(\log(n))$$

◀

Note that this corollary would apply equally well to any dynamics where the number of particles remains constant and the size of the graph grows polynomially (not necessarily as a square root).

The asymptotic regime of the size function was reached as soon as all the merger patterns were destroyed, cf. Fig. 4a. The same happens with global entropy, cf. Fig. 4b.

If we are only interested in whether entropy grows, without seeking to characterise its asymptotic behaviour, we can state a more general theorem, relating it to size growth. Indeed, under the assumption that the particles do not fill the whole space, nor disappear completely, then any dynamics that increase the size of the graph will also increase the entropy:

► **Theorem 9** (Entropy increases with size). *For all $X \in \mathcal{C}_u$ and $f : \mathcal{C}_u \rightarrow \mathcal{C}_u$ such that :*



- $\lim_{n \rightarrow +\infty} |V(f^n(X))| = +\infty$
- $\exists m \in \mathbb{N}$ such that $\forall n \geq m, 1 \leq p_n \leq 2u \times |V(f^n(X))| - 1$ where p_n is the number of particles in the step in $f^n(X)$.

We have that $\lim_{n \rightarrow +\infty} S'(f^n(X)) = +\infty$.

Proof. Thanks to the second condition, we have for all $n \geq m$:

$$S'(f^n(X)) = \log\left(\binom{n}{p}_{|V(f^n(X))|}\right) \geq \log\left(\binom{|V(f^n(X))|}{1}\right) = \log(|V(f^n(X))|)$$

As $\log(|V(f^n(X))|)$ tends to $+\infty$ when n tends to $+\infty$, this is also the case for $S'(f^n(X))$. \blacktriangleleft

3.5 Recovering an arrow of time

With Th. 7 and Cor. 3.1, we have proven that an entropic arrow of time emerges in some reversible, causal, homogeneous reversible laws (namely the $\sqrt{\tau}I$ toy model), without relying on the past hypothesis. More precisely, we have proven that starting from generic configurations, entropy ultimately grows as we iterate the dynamics. Intuitively, after a finite period of dynamical clock time, the entropic clock's arrow aligns with that of the dynamical clock. This solves criticism (iii) of the conventional argument. Notice how, ultimately, this resolution boils down to the fact that configurations are of finite but unbounded size. In this context, assuming that the universe “starts small” is reasonable, because for any configuration, there are many more larger configurations than smaller ones. The same happens with entropy: any starting value is small within the set of positive real numbers. In that sense past low entropy is no longer unreasonable, it is unavoidable.

An immediate consequence is that the toy model is not periodic, i.e. there is no recurrence time: this solves criticism (i) in a way more satisfactory manner than arguing that “there is a recurrence time but it is typically too big to be observed”. Let us look at criticism (ii).

Since the system $\sqrt{\tau}I$ is reversible, one can naturally ask what happens if one tries to “go back in time”, i.e. how a generic graph evolves when one applies the dynamics $(\sqrt{\tau}I)^{-1} = I^{-1}\sqrt{\tau}^{-1}$. Numerics suggest it also increases the size of the graph, but at a different rate, see Fig. 6a. We can prove it:

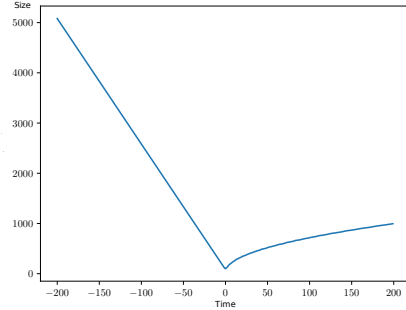
► **Theorem 10.** *For any $X \in \mathcal{C}_1$ containing at least one particle of each type, the sequence $(|V((\sqrt{\tau}I)^{-n}(X))|)_{n \in \mathbb{N}}$ is of the order of n .*

Proof. In the absence of patterns  , the size of the graph decreases strictly each time two particles meet. By conservation of momentum, the particles will continue to cross each other. Since the graph cannot decrease continuously a pattern  will inevitably form. As can be seen in the proof of Lem. 5, the pattern  is stable by $I^{-1}\sqrt{\tau}^{-1}$, and cannot be crossed by other particles. This implies that once such a pattern is present, any pair of particles not belonging to such a pattern can only collide once. When all these collisions have occurred, each application of $I^{-1}\sqrt{\tau}^{-1}$ increases the size of the graph by the number of patterns present. We can bound by $\min(n_a, n_b)$ the number of such patterns in X and its successors by $I^{-1}\sqrt{\tau}^{-1}$. Thus there exists $m \in \mathbb{N}$ such that for all $n \geq m$ we have :

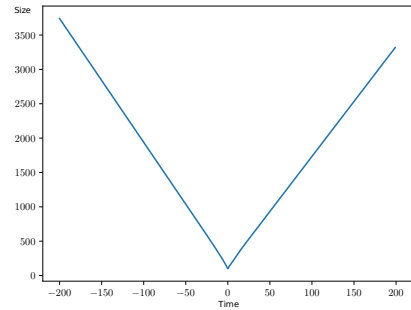
$$|V((\sqrt{\tau}I)^{-m}(X))| + n \leq |V((\sqrt{\tau}I)^{-n}(X))| \leq |V((\sqrt{\tau}I)^{-m}(X))| + n \times \min(n_a, n_b)$$

\blacktriangleleft

By the same proof scheme as for corollary 3.1, we obtain the entropy growth for $I^{-1}\sqrt{\tau}^{-1}$:



(a) Typical curve of size of the graphs under $(\sqrt{\tau}H)^{-1}$ and $\sqrt{\tau}H$. The initial condition is drawn uniformly at random amongst graphs of size 100. We run the dynamics backwards and forward to explore negative and positive dynamical clock times.



(b) Typical curve of size of the graphs under $\sqrt{\tau}I_2$. The initial condition is drawn uniformly at random amongst graphs of size 100, thus particle density is high ~ 0.5 .

► **Corollary 3.2.** For any $X \in \mathcal{C}_1$ containing at least one particle of each type, the sequence $(S'(\sqrt{\tau}I)^{-n}(X))_{n \in \mathbb{N}}$ is of the order of $\log(n)$.

Thus, a variation of criticism (ii) still holds, as entropy increases in both directions from a ‘source’. But here, since the model is not periodic, there is a single such source: a possibility discussed under the name of ‘Janus point’ [14, 15, 9, 8]. To move away from this region of minimal entropy, whether by iterating the forward dynamics or its reverse, means augmenting entropy and hence ‘going towards the future’. The important point is the way in which this variation relates to the resolution of criticism (iii): it is no longer necessary to assume that the universe “started” in an improbable low-entropy state; as the existence of an arrow of time just follows from the existence of a minimal region, which itself is a direct consequence of the dynamical law.

4 Time-symmetric model

Although the $\sqrt{\tau}I$ toy model is reversible, it is not time-symmetric:

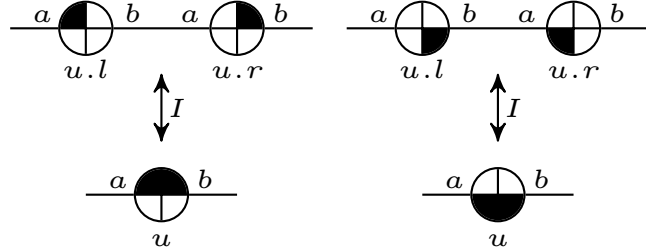
► **Remark 4.1.** If f is temporally symmetric by T then for all $n \in \mathbb{N}, Tf^nT = f^{-n}$. Consequently, since $\sqrt{\tau}I$ and $I^{-1}\sqrt{\tau}^{-1}$ do not have the same asymptotic behaviour, they are not temporally symmetric.

However, there is a way to time-symmetrize the dynamics, by extending the state space to 2 bits of information per port, i.e. by working on \mathcal{C}_2 . First of all notice that step $\sqrt{\tau}$ is already defined for an arbitrary \mathcal{C}_n , and time-symmetric under conjugation by the involution T . We only need to extend step I , because although I is not time-symmetric under conjugation by that same conjugation T . Indeed, the orientation of the particles affects the behaviour of I : a pattern may merge or not depending on whether we apply T .

We thus time-symmetrize step I into step I_2 , adding 2 bits of information, for which step I_2 will trigger split/mergers, not on $\text{--} \bullet \text{--} \bullet \text{--}$, but on $\text{--} \bullet \text{--} \bullet \text{--}$, as in Fig. 7. In other words, step I_2 acts on the second bit, just like TIT would act on the first bit.

► **Proposition 11.** *The dynamics $\sqrt{\tau}I_2$ is time-symmetric.*

Proof. We define the function $R : \mathcal{C}_2 \rightarrow \mathcal{C}_2$ which for any vertex u exchanges the values of $a_1(u)$ and $b_2(u)$, as well as the values of $a_2(u)$ and $b_1(u)$. One can easily verify that such



■ **Figure 7** Dynamics I_2 . The presence of a particle is represented in black. Now there are two types of particles corresponding to port a , and two corresponding to port b .

a dynamic commutes with I_2 , i.e. that $I_2R = RI_2$. Moreover, since R exchanges particles on the ports a and b , we have that $R\sqrt{\tau}R = \sqrt{\tau}^{-1}$. By letting $T := I_2R$, we obtain the equalities:

$$T^2 = I_2RI_2R = I_2I_2RR = \text{Id}$$

And also :

$$T\sqrt{\tau}I_2T = I_2R\sqrt{\tau}I_2I_2R = I_2R\sqrt{\tau}R = I_2\sqrt{\tau}^{-1} = I_2^{-1}\sqrt{\tau}^{-1}$$

◀

The symmetry comes at a price: with potentially 2 types of particles per node, interactions through step I_2 are sometimes prevented in a way that makes it difficult to extend Th. 7. Still, we have strong numerical evidence that generic graphs expand, with a size curve of order $\Theta(n)$, see Fig. 6b.

Just like for $\sqrt{\tau}I$, the system has a minimal configuration from which two time arrows pointing in opposite directions are derived. In our experiments, this configuration is often the initial configuration. This does not mean that it is non-generic, quite the contrary: by drawing a configuration uniformly at random from the set of graphs of a certain size, we obtain with high probability a density that is close to 2 particles per node. On the other hand, if we were to randomly choose a configuration X from the set of configurations of an orbit, then for all $\epsilon \in [0, 1]$, the density of X would be less than ϵ with probability 1 (if it is indeed true that the size of the graph grows in $\Theta(n)$ that is). By lowering the particle density of the initial state, we lower its chances of being the minimal configuration, see Fig. 8.

5 Exponential growth models

The very early universe is believed to have known a phase of exponential growth, called inflation. Is this compatible with reversibility? Intuitively, we can achieve this in a variant of our toy model if the growth of the configuration is made proportional to the size of the configuration. This was not the case with $\sqrt{\tau}I$ because it preserves the number of particles. This will be fixed if we manage to maintain the particle density above a certain limit. There are two simple ways of doing so.

The first is to create new particles at each node division, for example by replacing step I with the step I_e shown in Fig. 9a. Under dynamics $\sqrt{\tau}I_e$, the particle density tends towards 1/2, which naturally leads to exponential growth according to numerics, see Fig. 10a.

The other possibility is to flip all the information bits of each vertex at each iteration, via step F , as illustrated in Fig. 9b. Dynamics $F\sqrt{\tau}I$ does not actually keep the particle

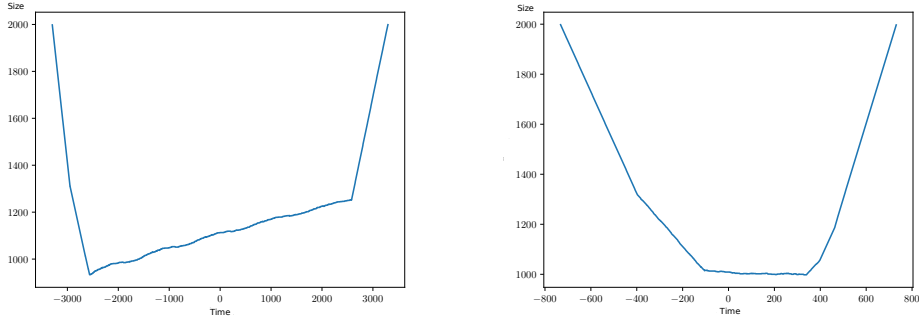
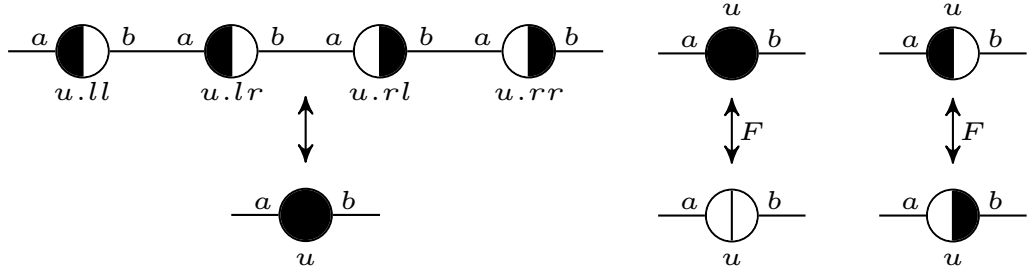
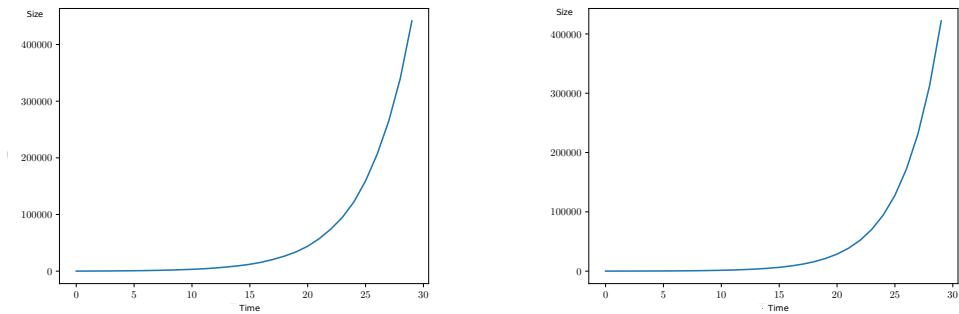


Figure 8 Typical curve of size of the graphs under $\sqrt{\tau}I_2$, starting from low density initial conditions. The initial condition is drawn at random amongst low density graphs of size 1000, in such a way that each bit be set with probability 0.01. Time 0 is chosen a posteriori, so that size 2000 be reached. A chaotic phase is followed by linear growth.



(a) Step I_e . Particles crossing crossing on a vertex trigger a split into a pattern of 4 vertices, thereby creating 2 new particles.

(b) Dynamics F .



(a) Typical curve of size of the graphs under $\sqrt{\tau}I_e$. The initial condition is drawn uniformly at random amongst graphs of size 100 and density ~ 0.1 .

(b) Typical curve of size of the graphs under $\sqrt{\tau}IF$. The initial condition is drawn uniformly at random amongst graphs of size 100.

density above a bound, but it does oscillate between more or less than 1 particles per vertex. This ensures that at least every second iteration, density is above $\frac{1}{2}$. Again this leads to exponential growth according to numerics, see Fig. 10b.

6 Fighting thermal death

The previous sections provide a plausible toy model explanation for the entropic clock's arrow of time at global scales. But, is this explanation good enough to also explain the arrow of time that we observe locally, at our scales, e.g. going back to the glass of water with a drop of dye of Sec. 2? The fact is that local entropy quickly drops close to zero in the toy model, due to the dilution of matter under expansion. This is also the dominant process in cosmology, where it is known as 'thermal death' (aka "big freeze"). This section provides a mechanism for whereby clumps of matter form, slowing down thermal death. That way local entropy still can increase at places, and the arrow of time be witnessed locally.

6.1 Prognosis

Local entropy dies out

In order to define a notion of local entropy entropy we apply the previous notion to disks of radius r of the configuration. Here we average that:

► **Definition 12** (Average local entropy). *Let S be an entropy function on \mathcal{X} , and $r \in \mathbb{N}^+$. The average local entropy function of radius r is defined by :*

$$S_r(X) := \frac{1}{|V(X)|} \sum_{u \in V(X)} S(X_u^r)$$

The average local entropy turns out to be bounded by the density of the graph:

► **Theorem 13.** *For all graphs X and for all $r \in \mathbb{N}$: $S_r(X) \leq r \frac{p(X)}{|V(X)|}$, where $p(X)$ is the number of particles of X .*

Proof.

$$\begin{aligned} S_r(X) &= \frac{1}{|V(X)|} \sum_{u \in V(X)} S(X_u^r) \\ &= \frac{1}{|V(X)|} \left(\sum_{\substack{u \in V(X) \\ p(X_u^r) > 0}} S(X_u^r) + \sum_{\substack{u \in V(X) \\ p(X_u^r) = 0}} S(X_u^r) \right) \\ &= \frac{1}{|V(X)|} \sum_{\substack{u \in V(X) \\ p(X_u^r) > 0}} S(X_u^r) \\ &\leq \frac{1}{|V(X)|} \times r p(X) \end{aligned}$$

◀

If the dynamics grows the size of the graph whilst preserving the number of particles, we cannot escape thermal death:

► **Corollary 6.1** (Thermal death). For any dynamics F that has a bounded number of particles and increasing graph sizes, for all $r \in \mathbb{N}$: $\lim_{n \rightarrow +\infty} S_r(F^n(X)) = 0$

At first glance this result may seem to go against our everyday experience, whereby we witness an arrow of time locally. Yet it is also true that as the Universe expands, it becomes mostly empty, and its average local entropy drops: thermal death is one of the envisaged fates for the Universe.

Corollary 6.1 is verified numerically for dynamics $\sqrt{\tau}I$ in Fig. 11 as well as for the time-symmetrized variant and their reverse dynamics. In the case of $(\sqrt{\tau}I)^{-1}$, we can show that after a certain time, stable patterns are formed that keep on producing new vertices. The other particles cannot cross these patterns, they end up constantly moving in the same direction and thus not crossing each other (dynamics $\sqrt{\tau}I_2$ seems to behave likewise).

In order to still witness growth in local entropy, in spite of expansion, average local entropy for fixed-size windows is therefore not the right mathematical quantity. We must look for a quantity which compensates for the loss of particle density. One way to proceed is to study average local entropy for variable-size windows, whose size follow expansion. This is done in Appendix D. Next, we study the sum of the local entropies for fixed-size windows, instead.

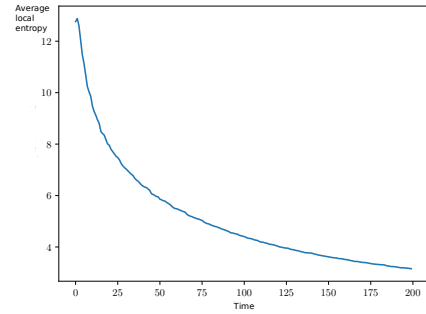
The sum of local entropies reaches a plateau

Recall that the local entropy of a fixed-sized window is directly related to the density of particles there. Thus, generally speaking: 1/ local entropy drops as the density drops and 2/ once the density is everywhere very low, the local entropy can only increase by gaining particles from the neighbouring window, whose entropy then decreases. I.e. local entropy at this stage is mostly just moving around alongside with the particles. Instead, we wish to have a mathematical quantity that allows us to monitor local entropies in a way that 1/ factors out the dilution of matter and 2/ ignores mere displacements from one window to the next. This all suggests studying the sum of local entropies:

$$\overline{S}_r(X) = \sum_{u \in V(X)} S(X_u^r)$$

Unfortunately, the sum of the entropies grows only very briefly for our previous dynamics, before it reaches the plateau of death, as seen in Fig. 12.

Details per models. Dynamics $\sqrt{\tau}I_2$ and $(\sqrt{\tau}I)^{-1}$, behave similarly: the growth in local entropy around the time 0 is the consequence of the growth of the graph. Then, division patterns fragment the space between the particles, and prevent any interaction. Thus, one essentially obtains patterns moving away at constant speed, between which inactive patterns move. This can be easily seen on a spacetime diagram on which the particles and the local entropy are superimposed (see Fig. 3b). Dynamics $\sqrt{\tau}I$ has a different behaviour. Observe



■ **Figure 11** Typical curve of average local entropy of the graphs under $\sqrt{\tau}I$. The initial condition is drawn uniformly at random amongst graphs of size 100.

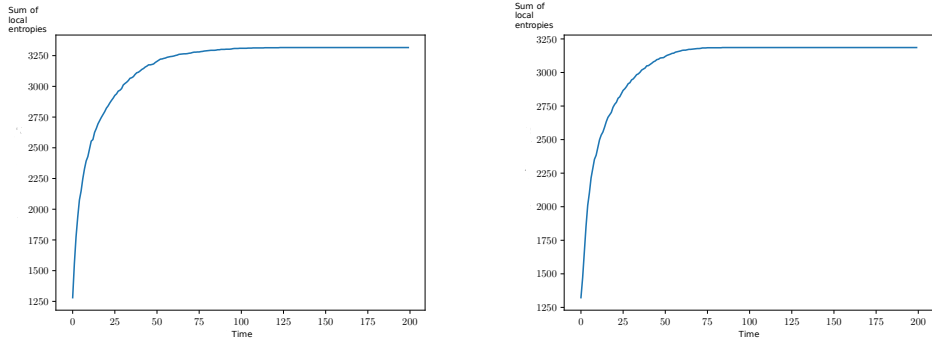


Figure 12 Typical curves of the sum of the local entropies of the graphs under $\sqrt{\tau}I$ and $\sqrt{\tau}I_2$. The local entropy windows are of radius 5. The initial conditions are drawn uniformly at random amongst graphs of size 100.

that the sum of local entropy reaches its maximum when each local window contains at most one particle in each direction. Once all merger patterns are destroyed, each time a particle collides with another, the distance between it and the other particles with the same orientation increases. Thus, for local entropy windows of radius r , the maximum sum of local entropy will be reached once each particle has completed $2r$ revolutions.

6.2 Treatment

In order to preserve the possibility of local entropy growth over a longer period of dynamical clock time, we need extra ingredients. There are many avenues that could be explored and nature-inspired models [24, 23] do not seem entirely out of reach, but they would require modelling efforts that lie beyond the scope of this paper, and whose complexity would likely obscure its main message. Still, some of the key ingredients seem to be matter clumping and radiation, and we can easily start to introduce these by implementing ‘inelastic shocks’.

Inelastic shocks

To do so we use 2 bits of information per port, i.e. state space \mathcal{C}_2 , and consider the composition of dynamics $\sqrt{\tau}$ which we already defined, with D_l and D_r which we introduce. D_r is defined to be the permutation the 4 different patterns shown in Fig. 14 (it acts as the identity on all other patterns). D_l is the left-right-symmetric of D_r , as obtained by 1/ inverting the position of nodes u and v and their contents 2/ inside each node, inverting the positions of the particles between ports a and b .

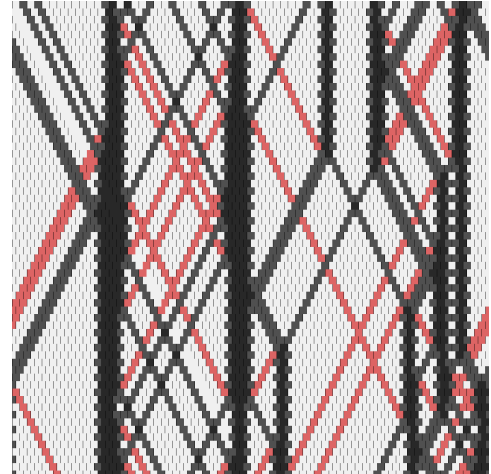


Figure 13 Spacetime diagram of $\sqrt{\tau}D$. Matter particles are shown in levels of grey, radiation particles are shown in red. For readability purposes, the initial configuration was taken without radiation.

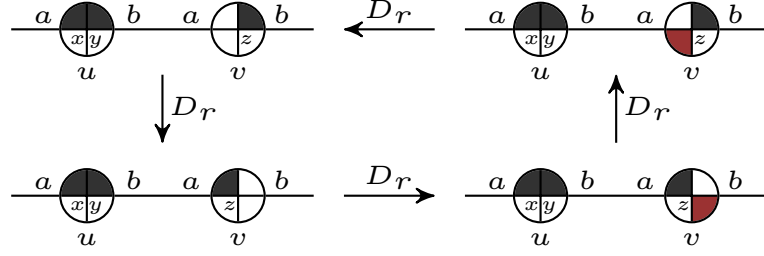


Figure 14 Dynamics D_r . ‘matter particles’ are shown in black. ‘radiation particles’ are shown in red. The x, y, z are boolean variables, so that the rule can apply independently of the presence or absence of these particles. Any left-incoming matter particle (bottom-right) gets stuck emitting radiation (bottom-right). From there on the clump is stable: any right-outgoing particle (top-left) is brought back (bottom-left). It will only be freed by left-incoming radiation particles (top-right).

Fig. 13 shows the evolution of a configuration under the dynamics $\sqrt{\tau}D$. Intuitively, D_l and D_r allow particles encoded by the first information bit (‘matter particles’) to clump together by emitting particles encoded by the second information bit (‘radiation particles’). Conversely, when an clump of matter gets hit by a radiation particle, the radiation particle is absorbed, and a matter particle separate. This is analogous to an inelastic shock, where the collision of two massive objects lets the kinetic energy due to their relative velocity dissipate into heat. Similarly, radiation will erode an object. We write $D := D_l D_r$.

Next, we combine inelastic shocks with our previous ability to shrink/expand the graph, just by placing ourselves in \mathcal{C}_3 i.e. adding a 3rd bit of information per port, on which the toy model dynamics $\sqrt{\tau}I$ operates. In order not to interfere with other particles types, we just restrict I to apply if and only if the neighbourhood does not contain matter nor radiation particles, and call this I_3 . Fig. 15a shows the spacetime diagram starting from a configuration containing no radiation particle, and density $\frac{1}{4}$ for the other particles. Fig. 15b instead starts from a configuration saturated with radiation particles: notice how it ends up with fewer matter clumps.

Conservation law

The following conservation law establishes a relation between the size of the matter clumps, and the level of radiation .

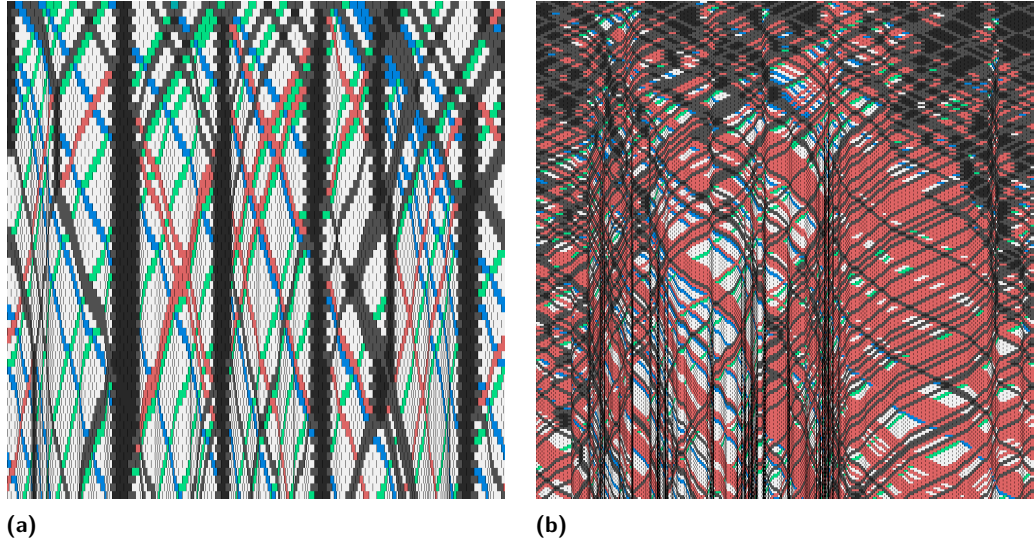
► **Theorem 14.** *For all $X \in \mathcal{C}_2$, $E(\sqrt{\tau}D(X)) = E(X)$ where E is defined by :*

$$E(X) := \sum_{u \in V(X)} (a_1(u)a_1(u.b)b_1(u.b) + b_1(u)a_1(u.a)b_1(u.a)) - \sum_{u \in V(X)} (a_2(u) + b_2(u))$$

i.e. the number of matter particles that are such that the neighbour on the opposite port contains two matter particles, minus the number of radiation particles, is constant.

Proof. (Outline). The proof technique is step-by-step and case-by-case keeping track of E , thus akin to a program-invariant proof. We shift it to Appendix C for readability. ◀

Details on the model. From this conservation law we deduce that the number of particles can only ever vary within a factor of two with respect to that present initially. This provides a bound on the sum of local entropies.



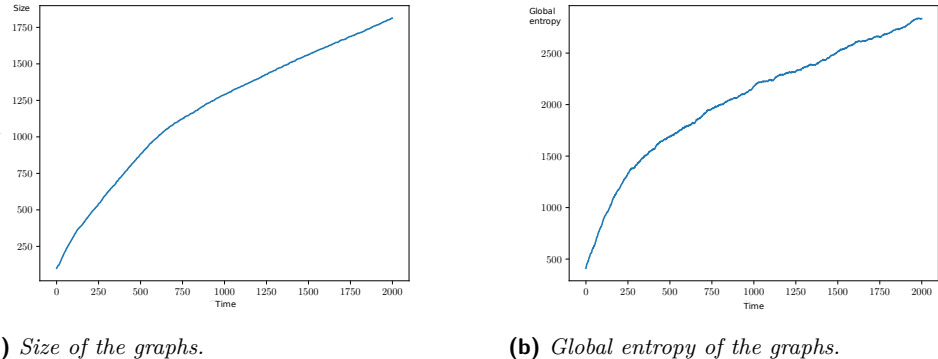
■ **Figure 15** Spacetime diagram of dynamics $\sqrt{\tau}ID$. Matter particles are shown in levels of grey, radiation particles are shown in levels of red. The particles responsible for expansion are shown in green and blue.

► **Corollary 6.2.** We have that for all $X \in \mathcal{C}_3$, and for all $n \in \mathbb{N}$, $p(X)/2 \leq p((\sqrt{\tau}I_3D)^n(X)) \leq 2 \times p(X)$, where $p(X)$ is the number of particles of X . Consequently, $\bar{S}_r(\sqrt{\tau}I_3D)^n(X)) \leq \sum_{i=0}^{2 \times p(X)} \log(\binom{2r+1}{i}) = 2 \times p(X) \times \log(2r+1)$.

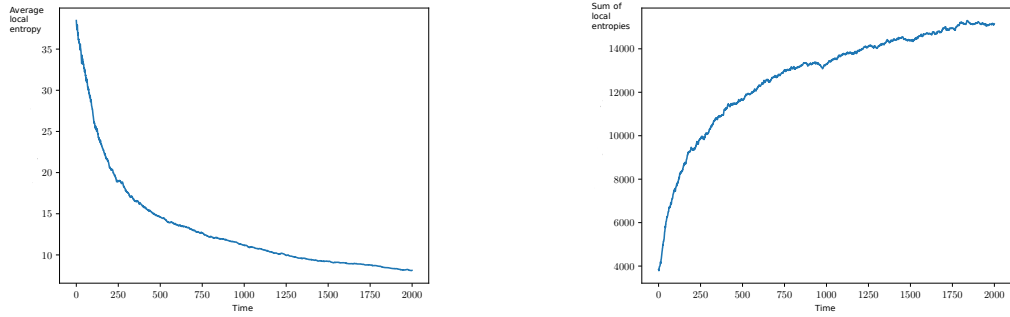
From this lower and upper bound on the number of particles it also follows from Th. 9 and Cor. 6.1 that for any graph X such that $(|V((\sqrt{\tau}I_3D)^n(X))|)_{n \in \mathbb{N}}$ is strictly increasing, the global entropy tends to $+\infty$ and the average local entropy tends to 0.

6.3 Trials

Again the complexity of $\sqrt{\tau}D$ comes at a price, with potentially 3 types of particles per nodes interactions through step I_3 are sometimes prevented in a way that makes it difficult to extend Th. 7. Still, we again have strong numerical evidence that generic graphs expand,



■ **Figure 16** Typical size and global entropy curves for dynamics $\sqrt{\tau}ID$. The initial condition is drawn uniformly at random amongst graphs of size 100.



(a) Average local entropy of the graphs.

(b) Sum of the local entropies of the graphs.

Figure 17 Typical local entropy curves for dynamics $\sqrt{\tau}ID$. The initial condition is drawn uniformly at random amongst graphs of size 100.

with a size curve of order $\Theta(\sqrt{n})$ matching that of the underlying dynamics of $\sqrt{\tau}I$ that is driving the growth, cf. Fig. 16a. Typically, other particles seem to only slightly slow down this growth, and may only totally prevent it in extreme cases. Again, as a result of this growth, global entropy grows (Fig. 16b) and average local entropy dies out (Fig. 17a). Again the sum of the local entropies reaches a plateau (Fig. 17b). Now, the interesting point is that it reaches is much more slowly.

The origin of this slower growth can be understood thanks to the conservation law of Th. 14. The inelastic shocks create matter clumps of not-so-low density, where enough degrees of freedom survive so as to preserve the possibility for local entropy growth within these matter-populated regions. This however, by the conservation law, is done at the cost of the emitting radiation particles (which increases the entropy of other local windows). The formation of a clump of matter is therefore temporary, lasting only as long it is not collided by a emitted radiation particles (cf. Fig. 15b). But as the graph size grows, radiation density lowers, and so the radiation travel times are longer. It follows that matter clumps survive for longer and longer, thereby preserving the possibility for local entropy growth for longer and longer.

This mechanism gets amplified when replacing the underlying growth dynamics $\sqrt{\tau}I$, with $\sqrt{\tau^{-1}}I^{-1}$, or with exponentially growing dynamics like $\sqrt{\tau}I_e$ and $F\sqrt{\tau}I$. For such dynamics, emitted radiation particles typically never make it back to the matter clumps, which act as stable ‘entropy reservoirs’.

7 Conclusion

This paper provides the first rigorous proof that an arrow of time typically emerges in some reversible dynamics, without the need for a past hypothesis. The reversible dynamics in question is cast in the setting of reversible causal graph dynamics ; the methods used pertain to the field of theoretical Computer Science. The proof works by showing that graph size increases, and that entropy increases with size, where entropy is defined as for perfect gases. It provides a local explanation for the origin of the arrow of time, by tracing it back to local, reversible expansion mechanisms acting over configurations of finite but unbounded size. This explanation resolves two of the three main criticism to the standard of the standard Boltzmann argument: there is no recurrence time, and no need to assume atypical initial conditions. One criticism still holds as there are successive configurations of minimal entropy

from which two arrows of time flow in opposite directions. This idea is present in some cosmological models and popularized under the name or ‘Janus point’.

We also show, numerically, that the explanation is compatible with fully time-symmetric dynamics, as well as periods of exponential growth.

In thermodynamics entropy increases globally, but locally in may well decrease and stabilize close to zero, reaching the so-called ‘thermal death’. At which stage it becomes impossible to witness an arrow of time locally. This is expected, and does occur in the toy model. Indeed as the graph expands, global entropy increases without bound, because “there are more ways in which to position the matter”, but as the same time matter dilutes. In any fixed-sized window, matter becomes scarce, there are less ways to position it, and so local entropy decreases. The sum of the local entropies still increases as it should, but soon it stabilizes around an upper bound, characteristic of thermal death. All too quickly, there is no longer enough matter for the local entropy to increase; there is nowhere in the graph where we are able to observe an arrow of time locally. This is somewhat unrealistic. Although our universe, ~ 13.7 billion years after the big bang, is indeed largely empty, it still has regions where enough matter is concentrated so that local entropy may continue to increase, allowing us to observe local entropic clocks. According to Reichenbach and Rovelli [24, 23] this is mainly due to the clumping of matter and the emission of radiation, through a delicate interplay between nucleosynthesis and gravity: modelling such processes lied way beyond the scope of this paper and therefore belongs to the perspectives. Yet, we provided numerical evidence that just by adding inelastic collisions of matter to the model (and triggering the emission of radiation into free space so as to keep things reversible) the sum of the local entropies increases way slower. Locally, we are able to observe an arrow of time for longer. Thermal death is delayed.

Two other perspectives are: 1/ the study of the possibility of the emergence of a low curvature three-dimensional space from such reversible causal graph dynamics, and the study of entropy therein and 2/ the study of other notions of entropy such as metric entropy, topological entropy, or Von Neumann entropy in the quantum regime.

References

- 1 David Z Albert. Time and chance, 2001.
- 2 Pablo Arrighi. An overview of quantum cellular automata. *Natural Computing*, 18:885, 2019. arXiv preprint arXiv:1904.12956.
- 3 Pablo Arrighi, Marios Christodoulou, and Amélia Durbec. On quantum superpositions of graphs, no-signalling and covariance. *CoRR*, abs/2010.13579, 2020.
- 4 Pablo Arrighi, Amélia Durbec, and Matt Wilson. Quantum networks theory. *CoRR*, abs/2110.10587, 2021.
- 5 Pablo Arrighi, Amélia Durbec, and Aurélien Emmanuel. Reversibility vs local creation/destruction. In Michael Kirkedal Thomsen and Mathias Soeken, editors, *Reversible Computation - 11th International Conference, RC 2019, Lausanne, Switzerland, June 24-25, 2019, Proceedings*, volume 11497 of *Lecture Notes in Computer Science*, pages 51–66. Springer, Springer, 2019.
- 6 Pablo Arrighi, Nicolas Durbec, and Aurélien Emmanuel. Reversibility vs local creation/destruction. In *Proceedings of RC 2019, LNCS*, volume 11497, pages 51–66. Springer, 2019.
- 7 Pablo Arrighi, Simon Martiel, and Vincent Nesme. Cellular automata over generalized cayley graphs. *Mathematical Structures in Computer Science*, 28(3):340–383, 2018.
- 8 Julian Barbour. *The Janus point: A new theory of time*. Random House, 2020.
- 9 Julian Barbour, Tim Koslowski, and Flavio Mercati. Identification of a gravitational arrow of time. *Phys. Rev. Lett.*, 113:181101, Oct 2014.

- 10 Julian Barbour, Tim Koslowski, and Flavio Mercati. Janus points and arrows of time. *arXiv preprint arXiv:1604.03956*, 2016.
- 11 Ludwig Boltzmann. *Vorlesungen Über Gastheorie*. Barth, Leipzig, 1. auflage edition, 1896.
- 12 Ludwig Boltzmann. *Lectures on gas theory*. Courier Corporation, 2012.
- 13 Latham Boyle, Kieran Finn, and Neil Turok. Cpt-symmetric universe. *Physical review letters*, 121(25):251301, 2018.
- 14 Sean M Carroll and Jennifer Chen. Spontaneous inflation and the origin of the arrow of time. *arXiv preprint hep-th/0410270*, 2004.
- 15 Sean M Carroll and Jennifer Chen. Does inflation provide natural initial conditions for the universe? *International Journal of Modern Physics D*, 14(12):2335–2339, 2005.
- 16 Shagnik Das. A brief note on estimates of binomial coefficients. <https://www.semanticscholar.org/paper/A-brief-note-on-estimates-of-binomial-coefficients-Das-e0e703e1bbc914e563afb72480d7f915df79b834>, 2015.
- 17 Anahí Gajardo, Jarkko Kari, and Andrés Moreira. On time-symmetry in cellular automata. *Journal of Computer and System Sciences*, 78(4):1115–1126, 2012.
- 18 Sheldon Goldstein, Roderich Tumulka, and Nino Zanghì. Is the hypothesis about a low entropy initial state of the universe necessary for explaining the arrow of time? *Phys. Rev. D*, 94:023520, Jul 2016.
- 19 J. Hardy, Y. Pomeau, and O. de Pazzis. Time Evolution of a Two-Dimensional Classical Lattice System. *Physical Review Letters*, 31(5):276–279, July 1973.
- 20 J. B. Hartle and S. W. Hawking. Wave function of the universe. *Phys. Rev. D*, 28:2960–2975, Dec 1983.
- 21 Brosl Hasslacher and David A. Meyer. Modelling dynamical geometry with lattice gas automata. Expanded version of a talk presented at the Seventh International Conference on the Discrete Simulation of Fluids held at the University of Oxford, June 1998.
- 22 Tim A Koslowski, Flavio Mercati, and David Sloan. Through the big bang: Continuing einstein’s equations beyond a cosmological singularity. *Physics Letters B*, 778:339–343, 2018.
- 23 Carlo Rovelli. Where was past low-entropy? *Entropy*, 21(5), 2019.
- 24 Carlo Rovelli. Back to reichenbach. 2022.
- 25 AD Sakharov. Cosmological models of the universe with reversal of time’s arrow. *JETP*, 52:349–351, 1980.
- 26 C. E. Shannon. A mathematical theory of communication. *The Bell System Technical Journal*, 27(3):379–423, July 1948.
- 27 Alexander Vilenkin. Arrows of time and the beginning of the universe. *Physical Review D*, 88(4):043516, 2013.
- 28 Robert M. Wald. The arrow of time and the initial conditions of the universe. *Studies in History and Philosophy of Science Part B: Studies in History and Philosophy of Modern Physics*, 37(3):394–398, 2006. The arrows of time, 2006.
- 29 Christopher Gregory Weaver. On the carroll–chen model. *Journal for General Philosophy of Science*, 48(1):97–124, 2017.
- 30 H Dieter Zeh. Comment on the "janus point" explanation of the arrow of time. *arXiv preprint arXiv:1601.02790*, 2016.

A Named graphs

Say as in Fig. 2b that some quantum evolution splits a vertex u into two. We need to name the two infants in a way that avoids name conflicts with the vertices of the rest of the graph. But if the evolution is locally-causal, we are unable to just ‘pick a fresh name out of the blue’, because we do not know which names are available. Thus, we have to construct new names locally. A natural choice is to use the names $u.l$ and $u.r$ (for left and right respectively). Similarly, say that some other evolution merges two vertices u, v into one. A natural choice

is to call the resultant vertex $u \vee v$, where the symbol \vee is intended to represent a merger of names.

This is, in fact, what the inverse evolution will do to vertices $u.l$ and $u.r$ that were just split: merge them back into a single vertex $u.l \vee u.r$. But, then, in order to get back where we came from, we need that the equality $u.l \vee u.r = u$ holds. Moreover, if the evolution is reversible, then this inverse evolution does exist, therefore we are compelled to accept that vertex names obey this algebraic rule.

Reciprocally, say that some evolution merges two vertices u, v into one and calls them $u \vee v$. Now say that some other evolution splits them back, calling them $(u \vee v).l$ and $(u \vee v).r$. This is, in fact, what the inverse evolution will do to the vertex $u \vee v$, split it back into $(u \vee v).l$ and $(u \vee v).r$. But then, in order to get back where we came from, we need the equalities $(u \vee v).l = u$ and $(u \vee v).r = v$.

► **Definition 15** (Names). *Let \mathbb{K} be a countable set. The name algebra $\mathcal{N}[\mathbb{K}]$ has terms given by the grammar*

$$u, v ::= c \mid u.t \mid u \vee v \quad \text{with} \quad c \in \mathbb{K}, \quad t \in \{l, r\}^*$$

and is endowed with the following equality theory over terms (with ε the empty word):

$$(u \vee v).l = u \quad (u \vee v).r = v \quad u.\varepsilon = u \quad u.l \vee u.r = u$$

We define $\mathcal{V} := \mathcal{N}[\mathbb{K}]$.

The fact that this algebra is well-defined was proven in [6]. Now that we have a set of possible names for our vertices, we can readily define ‘port graphs’ (aka ‘generalized Cayley graphs’ [7]. Condition (1) will just ensure that names do not intersect, e.g. forbidding that there be a name $u \vee v$ and another $v \vee w$, so as to avoid name collisions should they split.

► **Definition 16** (Named graphs). *Let Σ be the set of internal states and π be the set of ports. A graph G is given by a finite set of vertices $V_G \subseteq \mathcal{V}$ such that*

$$v, v' \in S \text{ and } v.t = v'.t' \text{ implies } v = v' \text{ and } t = t' \tag{1}$$

together with

- $\sigma_G : V_G \rightarrow \Sigma$ its internal states
- E_G a set of non-intersecting two element subsets of $V_G : \pi$, its edges.

In other words an edge e is of the form $\{x : a, y : b\}$ and $\forall e, e' \in E_G, e \cap e' \neq \emptyset \Rightarrow e = e'$.

B Proof of Th. 7

Proof. First, it is argued that there is a time step m after which no more vertex mergers will occur. We denote $n_f(X)$ the number of merger patterns in X , and $d_f(X)$ the minimum distance between a merger pattern and a particle moving towards it (this includes a particle present in a merger pattern, and itself if there are no other particles). We will show that the pair $(n_f(\sqrt{\tau}I)^n(X), d_f(\sqrt{\tau}I)^n(X))$ decreases strictly in lexicographic order.

As we have seen in Lem. 5, a merger pattern cannot be created, and is destroyed on collision. We only need to prove that $d_{fu}((\sqrt{\tau}I)^n X)$ decreases strictly when $p(\sqrt{\tau}I)^n X$ remains constant. Let u, v be two vertices of a merger pattern and p a particle such that u, v and p realise the distance $d_f(X)$. Two cases can occur, either p is itself part of a merger pattern, in which case there are no particles between the two merger patterns, or p is free

moving, in which case there are only particles going in the opposite direction between p and u, v . In the first case, the two perform a fusion and there are no particles between the two merger patterns (so there is no division); the distance between the two patterns therefore decreases by 1. In the second case, the particle p will move towards the merger pattern, decreasing $d_{fu}((\sqrt{\tau}I)^n X)$.

In order to preserve the readability of the notations, we will denote (u_n) the sequence $(|V((\sqrt{\tau}I)^n(X))|)$. Thanks to the previous point, we know that there is a time step $m \in \mathbb{N}$ from which each collision of particles will cause the creation of an additional vertex, so the sequence u_n is necessarily increasing for all $n > m$. Since X contains at least one particle of each type, we have that for all $n \geq m$, the evolution of $(\sqrt{\tau}I)^n X$ during u_n time steps causes at least one collision. Similarly, we know that at most $c = 2n_a n_b$ collisions occur in the same time frame where n_a (resp. n_b) is the number of particles on the port a (resp. b). This allows us to obtain the following inequalities:

$$u_n + 1 \leq u_{n+u_n} \leq u_n + c \quad (2)$$

Let $(v_k)_{k \in \mathbb{N}}$ be the sub-sequence such that $v_0 = u_m$ and for all $k \in \mathbb{N}$, $v_{k+1} = u_{\text{ind}(k)+v_k}$, where $\text{ind}(k)$ is the function such that $\text{ind}(0) = m$ and for all $k \in \mathbb{N}$, $\text{ind}(k) = \sum_{i=0}^{k-1} v_i$. By recurrence, we prove that $u_{\text{ind}(k)} = v_k$:

$$u_{\text{ind}(k+1)} = u_{\sum_{i=0}^k v_i} = u_{v_k + \sum_{i=0}^{k-1} v_i} = u_{\text{ind}(k)+v_k} = v_{k+1} \quad (3)$$

This allows us to apply the inequality (2) on $v_{k+1} = u_{\text{ind}(k)+v_k}$. Combining (2) and (3), we obtain the linear growth of $(v_k)_{k \in \mathbb{N}}$:

$$v_k + 1 \leq v_{k+1} = u_{\text{ind}(k)+v_k} \leq v_k + c \quad (4)$$

Let us now focus on the growth of the index of $(v_k)_{k \in \mathbb{N}}$. By applying the inequalities of (4) to the definition of $\text{ind}(k)$ we obtain :

$$\sum_{i=0}^k (v_0 + i) \leq \sum_{i=0}^k (v_i) \leq \sum_{i=0}^k (v_0 + ci) \quad (5)$$

$$ku_m + \frac{k(k-1)}{2} = \sum_{i=0}^k (v_0 + i) \leq \text{ind}(k) \leq \sum_{i=0}^k (v_0 + ci) = ku_m + c \frac{k(k-1)}{2} \quad (6)$$

To conclude, let us return to the main sequence $(u_n)_{n \in \mathbb{N}}$. For a sufficiently large n , there exists $k \geq 4u_m + c$ such that :

$$\text{ind}(k) \leq n \leq \text{ind}(k+1)$$

This gives us, considering that $(u_n)_{n \in \mathbb{N}}$ is increasing, the previous equation (6) and that $k \geq 4u_m + c$ the following inequalities:

$$\text{ind}(k) \leq n \leq \text{ind}(k+1) \quad (7)$$

$$\Rightarrow ku_m + \frac{k(k-1)}{2} \leq n \leq (k+1)u_m + c \frac{k(k+1)}{2} \quad (8)$$

$$\Rightarrow k(2u_m + k - 1) \leq 2n \leq k(4u_m + c + ck) \quad (9)$$

$$\Rightarrow 2k^2 \leq 2n \leq (c+1)k^2 \quad (10)$$

$$\Rightarrow k \leq \sqrt{n} \leq \sqrt{\frac{(c+1)}{2}k} \quad (11)$$

$$\Rightarrow \sqrt{\frac{2}{c+1}}\sqrt{n} \leq k \leq \sqrt{n} \quad (12)$$

Since the sequence u_n is increasing, and using the inequalities (12) and (4), we can conclude with the following inequalities:

$$u_m + \sqrt{\frac{2}{c+1}}\sqrt{n} \leq u_m + k \leq v_k \leq u_n \leq v_{k+1} \leq u_m + c(k+1) \leq u_m + c + c\sqrt{n}$$

Thus, u_n is of the order of (\sqrt{n}) . \blacktriangleleft

C Proof of Th. 14

Proof. The function E' is defined by :

$$E'(X) := \sum_{u \in V(X)} a_1(u)a_1(u.a)b_1(u.a) + b_1(u)a_1(u.b)b_1(u.b) - \sum_{u \in V(X)} (a_2(u) + b_2(u))$$

This time, it amounts to counting the number of matter particles such that the neighbour on the same port contains two matter particles and deducing the number of radiation particles. Following this intuition, we introduce the localised energy functions E and E' such that for all $X \in \mathcal{C}_2$ and for all $u \in X$:

$$E(X, u) = a_1(u)a_1(u.b)b_1(u.b) + b_1(u)b_1(u.a)a_1(u.a) - a_2(u) - b_2(u)$$

and

$$E'(X, u) = a_1(u)a_1(u.a)b_1(u.a) + b_1(u)b_1(u.b)a_1(u.b) - a_2(u) - b_2(u)$$

This notation is justified by the equalities:

$$E(X) := \sum_{u \in V(X)} E(X, u)$$

and

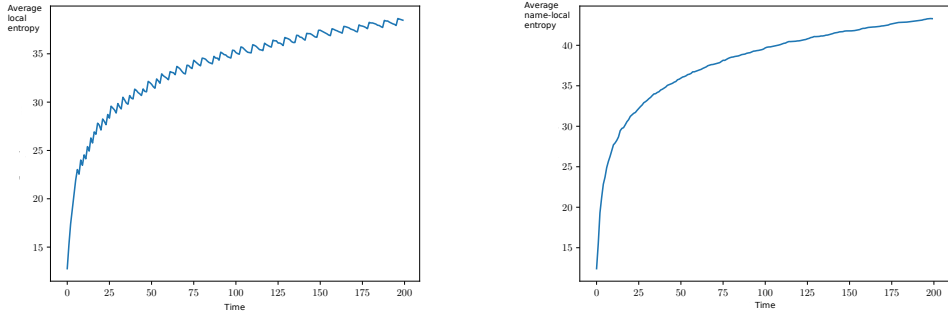
$$E'(X) := \sum_{u \in V(X)} E'(X, u)$$

Let us prove that for all X , we have $E(X) = E'(D(X)) = E(\sqrt{\tau}I_3D(X))$.

First, let us prove that $E(X, u) = E'(DX, u)$. By definition, D acts only in the neighbourhood of vertices u such as $a_1(u) = b_1(u) = 1$. Moreover, when D_l and D_r act on the same vertex v , we have by symmetry of the ports a and b that the vertex i is left unchanged by D . By the same symmetry, we can assume without loss of generality that only D_l affects vertex u , which gives us the following calculations:

$$\begin{aligned} E \left(\begin{array}{c} \text{---} \\ a \text{ } \bigcirc \text{---} \\ \text{---} \end{array} \begin{array}{c} b \\ | \\ x \text{---} y \end{array} \begin{array}{c} \text{---} \\ a \text{ } \bigcirc \text{---} \\ \text{---} \end{array} \begin{array}{c} b \\ | \\ z \end{array} \right) &= 1 - (x + y + z) &= E' \left(\begin{array}{c} \text{---} \\ a \text{ } \bigcirc \text{---} \\ \text{---} \end{array} \begin{array}{c} b \\ | \\ x \text{---} y \end{array} \begin{array}{c} \text{---} \\ a \text{ } \bigcirc \text{---} \\ \text{---} \end{array} \begin{array}{c} b \\ | \\ z \end{array} \right) \\ E \left(\begin{array}{c} \text{---} \\ a \text{ } \bigcirc \text{---} \\ \text{---} \end{array} \begin{array}{c} b \\ | \\ x \text{---} y \end{array} \begin{array}{c} \text{---} \\ a \text{ } \bigcirc \text{---} \\ \text{---} \end{array} \begin{array}{c} b \\ | \\ z \end{array} \right) &= -(x + y + z) &= E' \left(\begin{array}{c} \text{---} \\ a \text{ } \bigcirc \text{---} \\ \text{---} \end{array} \begin{array}{c} b \\ | \\ x \text{---} y \end{array} \begin{array}{c} \text{---} \\ a \text{ } \bigcirc \text{---} \\ \text{---} \end{array} \begin{array}{c} b \\ | \\ z \end{array} \right) \\ E \left(\begin{array}{c} \text{---} \\ a \text{ } \bigcirc \text{---} \\ \text{---} \end{array} \begin{array}{c} b \\ | \\ x \text{---} y \end{array} \begin{array}{c} \text{---} \\ a \text{ } \bigcirc \text{---} \\ \text{---} \end{array} \begin{array}{c} b \\ | \\ z \end{array} \right) &= -(x + y + z + 1) &= E' \left(\begin{array}{c} \text{---} \\ a \text{ } \bigcirc \text{---} \\ \text{---} \end{array} \begin{array}{c} b \\ | \\ x \text{---} y \end{array} \begin{array}{c} \text{---} \\ a \text{ } \bigcirc \text{---} \\ \text{---} \end{array} \begin{array}{c} b \\ | \\ z \end{array} \right) \\ E \left(\begin{array}{c} \text{---} \\ a \text{ } \bigcirc \text{---} \\ \text{---} \end{array} \begin{array}{c} b \\ | \\ x \text{---} y \end{array} \begin{array}{c} \text{---} \\ a \text{ } \bigcirc \text{---} \\ \text{---} \end{array} \begin{array}{c} b \\ | \\ z \end{array} \right) &= -(x + y + z) &= E' \left(\begin{array}{c} \text{---} \\ a \text{ } \bigcirc \text{---} \\ \text{---} \end{array} \begin{array}{c} b \\ | \\ x \text{---} y \end{array} \begin{array}{c} \text{---} \\ a \text{ } \bigcirc \text{---} \\ \text{---} \end{array} \begin{array}{c} b \\ | \\ z \end{array} \right) \end{aligned}$$

In summary, we have that $E(X) = E'(D(X))$. Similarly, for $\sqrt{\tau}$ we get :



(a) Average $r = 0.05$ -local entropy of the graphs.

(b) Average name-local entropy of the graphs for windows of size 5 initially.

■ **Figure 18** Typical of two modified average local entropy for the dynamics $\sqrt{\tau}I$. The initial condition is drawn uniformly at random amongst graphs of size 100.

$$E' \left(\begin{array}{c} \text{disk} \\ \text{c} \\ \text{disk} \end{array} \begin{array}{c} b \\ \text{a} \end{array} \begin{array}{c} \text{disk} \\ \text{c}_2 \text{c}_3 \\ \text{disk} \end{array} \begin{array}{c} b \\ \text{a} \end{array} \begin{array}{c} \text{disk} \\ \text{c}_4 \\ \text{disk} \end{array} \right) = m_1 + m_2 - (c_1 + c_2 + c_3 + c_4) \\ = E \left(\begin{array}{c} \text{disk} \\ \text{a} \\ \text{disk} \end{array} \begin{array}{c} b \\ \text{a} \end{array} \begin{array}{c} \text{disk} \\ \text{c}_4 \text{c}_3 \\ \text{disk} \end{array} \begin{array}{c} b \\ \text{a} \end{array} \right)$$

And so we get that $E'(X) = E(\sqrt{\tau}(X))$. Combining all this, we obtain that $E(X) = E'(D(X)) = E(\sqrt{\tau}D(X))$

◀

D Variable radius entropy

To still see a growth in local entropy, in spite of expansion, we need to compensate for the loss of particle density. There are two simple ways to do this. The first is to directly increase the radius of observation in proportion to the size of the graph, so that each disk always represents the same proportion of the graph, which will preserve the particle density. The other way is to use the names as markers to split the configurations into different induced subgraphs.

For the first case, it is sufficient to pose for $r \in [0, 1]$:

$$S'_r(X) := \frac{1}{|V(X)|} \sum_{u \in V(X)} S(X_u^{[r \times |V(X)|]})$$

This gives us an increasing entropy in the case of $\sqrt{\tau}I$, $(\sqrt{\tau}I)^{-1}$ and $\sqrt{\tau}I_2$ as can be seen in Fig. 18a.

Although it compensates for the expansion of the graph, this entropy makes little physical sense: a node creation on the opposite side of the graph can increase the size of a local window. To get rid of this problem, it is sufficient to use the name algebra as a coordinate system, and use them to determine whether two vertices belong to the same window. As the names of the vertices are in the algebra \mathcal{V} , they can be seen as finite binary trees labelled by $\mathbb{N}.\{l, r\}^*$. It is therefore sufficient to state that a window consists of the set of vertices whose leftmost child intersects the same integer. More formally, for all $i \in \mathbb{N}$, we pose:

$$V_i(X) = \{u \in V(X) \text{ et } \exists m \in \mathbb{N} \text{ tel que } u.l^m \wedge i = u.l^m\}$$

The average local entropy can then be defined as :

$$S_{\mathcal{N}}(X) := \frac{1}{|V(X)|} \sum_{i \in \mathbb{N}} S(X_{V_i}^0)$$

where n is the number of integers composing the names of X and $X_{V_i}^0$ is the subgraph induced by the set of vertices in $V_i(X)$.

This definition seems at first sight very restrictive, but it is important to remember that the dynamics of named graphs switch with any renaming. Thus, to observe how the local entropy evolves according to a different partitioning, we just need to rename the graph appropriately, and observe the entropy of the resulting graph.

Note that in this definition of entropy, local windows do not intersect. Moreover, a window only increases in size when the space inside it grows. This also makes physical sense to define entropy in this way: it is like placing a coordinate system in space and letting the dynamics distort it.

As for the previous definition of entropy, we always observe a local growth of entropy for the three dynamics mentioned above, illustrated in Fig. 18b.